AFRL-ML-WP-TP-2007-551

LIQUID CRYSTAL BRAGG GRATINGS: DYNAMIC OPTICAL ELEMENTS FOR SPATIAL LIGHT MODULATORS (POSTPRINT)

J.M. Wofford, D.R. Evans, and T.J. Bunning

Hardened Materials Branch
Survivability and Sensor Materials Division

JANUARY 2007

STINFO COPY

AIR FORCE RESEARCH LABORATORY
MATERIALS AND MANUFACTURING DIRECTORATE
WRIGHT-PATTERSON AIR FORCE BASE, OH 45433-7750
AIR FORCE MATERIEL COMMAND
UNITED STATES AIR FORCE

NOTICE AND SIGNATURE PAGE

AFRL-ML-WP-TP-2007-551 HAS BEEN REVIEWED AND IS APPROVED FOR PUBLICATION IN ACCORDANCE WITH ASSIGNED DISTRIBUTION STATEMENT.

*//Signature//

DEAN R. EVANS, Ph.D.
Agile Filters Project
Exploratory Development
Hardened Materials Branch

//Signature//

MARK S. FORTE, Acting Chief
Hardened Materials Branch
Survivability and Sensor Materials Division

//Signature//

TIM J. SCHUMACHER, Chief
Survivability and Sensor Materials Division

REPORT DOCUMENTATION PAGE

The public reporting burden for this collection of information is estimated to average 1 hour per response, including the time for reviewing instructions, searching existing data sources, searching existing data sources, gathering and maintaining the data needed, and completing and reviewing the collection of information. Send comments regarding this burden estimate or any other aspect of this collection of information, including suggestions for reducing this burden, to Department of Defense, Washington Headquarters Services, Directorate for Information Operations and Reports (0704-0188), 1215 Jefferson Davis Highway, Suite 1204, Arlington, VA 22202-4302. Respondents should be aware that notwithstanding any other provision of law, no person shall be subject to any penalty for failing to comply with a collection of information if it does not display a currently valid OMB control number. **PLEASE DO NOT RETURN YOUR FORM TO THE ABOVE ADDRESS.**

1. REPORT DATE *(DD-MM-YY)*	2. REPORT TYPE	3. DATES COVERED *(From - To)*
January 2007	Journal Article Postprint	

4. TITLE AND SUBTITLE
LIQUID CRYSTAL BRAGG GRATINGS: DYNAMIC OPTICAL ELEMENTS FOR SPATIAL LIGHT MODULATORS (POSTPRINT)

5a. CONTRACT NUMBER
In-house

5b. GRANT NUMBER

5c. PROGRAM ELEMENT NUMBER
62102F

6. AUTHOR(S)
R.L. Sutherland, V.P. Tondiglia, L.V. Natarajan, and S.A. Siwecki (Science Applications International Corporation)
J.M. Wofford, D.R. Evans, and T.J. Bunning (AFRL/MLPJ)
G. Cook (Universal Technology Corporation)
P.F. Lloyd (UES, Inc.)

5d. PROJECT NUMBER
4348

5e. TASK NUMBER
RG

5f. WORK UNIT NUMBER
M08R1000

7. PERFORMING ORGANIZATION NAME(S) AND ADDRESS(ES)

Science Applications International Corporation
Dayton, OH 45431

Hardened Materials Branch (AFRL/MLPJ)
Survivability and Sensor Materials Division
Materials and Manufacturing Directorate
Wright-Patterson Air Force Base, OH 45433-7750
Air Force Materiel Command, United States Air Force

Universal Technology Corporation
Dayton, OH 45432

UES, Inc.
Dayton, OH 45432

8. PERFORMING ORGANIZATION REPORT NUMBER
AFRL-ML-WP-TP-2007-551

9. SPONSORING/MONITORING AGENCY NAME(S) AND ADDRESS(ES)
Air Force Research Laboratory
Materials and Manufacturing Directorate
Wright-Patterson Air Force Base, OH 45433-7750
Air Force Materiel Command
United States Air Force

10. SPONSORING/MONITORING AGENCY ACRONYM(S)
AFRL/MLPJ

11. SPONSORING/MONITORING AGENCY REPORT NUMBER(S)
AFRL-ML-WP-TP-2007-551

12. DISTRIBUTION/AVAILABILITY STATEMENT
Approved for public release; distribution unlimited.

14. ABSTRACT
Bragg gratings yield a single diffracted order when irradiated by a coherent beam at the appropriate Bragg angle. In many cases, nearly all of the energy of the incident beam can be coupled to the diffracted beam. Hence these gratings can form many useful optical elements, and this has been realized in 1-D, 2-D, and 3-D photonic crystals. Bragg gratings made with liquid crystals offer the added dimension of dynamic properties through the large electro-optical effect in liquid crystals. Applications for spatial light modulators are numerous, including optical switches, modulators, active optical elements (e.g., lenses), laser sources, and tunable filters. We have been exploring a number of approaches for making liquid crystal Bragg gratings, including holographic polymer-dispersed liquid crystals, cholesteric liquid crystals, and homogenous nematic liquid crystals in hybrid devices. We have studied the dynamic properties of these Bragg gratings by electrical, thermal, and optical stimulation. Modification and control of optical and dynamic properties have been obtained through combinations of liquid crystals with polymers, combinations of various dopant materials, and interactions of liquid crystals with organic and inorganic interfaces. We discuss the materials, fabrication, characterization, and physics of liquid crystal Bragg gratings and present the results of various devices we have studied in our lab. We will also discuss potential applications.

15. SUBJECT TERMS spatial light modulators, Bragg gratings, liquid crystals

16. SECURITY CLASSIFICATION OF:			17. LIMITATION OF ABSTRACT:	18. NUMBER OF PAGES	19a. NAME OF RESPONSIBLE PERSON (Monitor)
a. REPORT Unclassified	**b. ABSTRACT** Unclassified	**c. THIS PAGE** Unclassified	SAR	20	Dean R. Evans
					19b. TELEPHONE NUMBER *(Include Area Code)* N/A

i

Liquid crystal Bragg gratings: Dynamic optical elements for spatial light modulators

R. L. Sutherland[*a,b], V. P. Tondiglia[a,b], L. V. Natarajan[a,b], J. M. Wofford[a], S. A. Siwecki[a,b], G. Cook[a,c], D. R. Evans[a], P. F. Lloyd[a,d] and T. J. Bunning[a]

[a]Air Force Research Laboratory (AFRL/MLPJ), Wright-Patterson Air Force Base, OH, USA 45433
[b]Science Applications International Corporation, Dayton, OH, USA 45431
[c]Universal Technology Corporation, Dayton, OH, USA 45432
[d]UES, Inc., Dayton, OH, USA 45432

ABSTRACT

Bragg gratings yield a single diffracted order when irradiated by a coherent beam at the appropriate Bragg angle. In many cases, nearly all of the energy of the incident beam can be coupled to the diffracted beam. Hence these gratings can form many useful optical elements, and this has been realized in 1-D, 2-D, and 3-D photonic crystals. Bragg gratings made with liquid crystals offer the added dimension of dynamic properties through the large electro-optical effect in liquid crystals. Applications for spatial light modulators are numerous, including optical switches, modulators, active optical elements (e.g., lenses), laser sources, and tunable filters. We have been exploring a number of approaches for making liquid crystal Bragg gratings, including holographic polymer-dispersed liquid crystals, cholesteric liquid crystals, and homogenous nematic liquid crystals in hybrid devices. We have studied the dynamic properties of these Bragg gratings by electrical, thermal, and optical stimulation. Modification and control of optical and dynamic properties have been obtained through combinations of liquid crystals with polymers, combinations of various dopant materials, and interactions of liquid crystals with organic and inorganic interfaces. We discuss the materials, fabrication, characterization, and physics of liquid crystal Bragg gratings and present the results of various devices we have studied in our lab. We will also discuss potential applications.

Keywords: spatial light modulators, Bragg gratings, liquid crystals

1. INTRODUCTION

A spatial light modulator (SLM) typically consists of a two-dimensional array of optical elements, or pixels, each of which can independently modulate the intensity, phase, or both of an incident optical beam. This produces a spatially varying modulation of the entire beam with control at the pixel level. Such devices are useful for delivering an image to a screen, for example in projection displays, or to a printer. However, the spatially modulated beam does not have to represent a visual image, but can also contain generic data. Thus, SLMs have also been proposed for use in direct-write lithography systems, holographic data storage, and optical computing.

Two types of SLM that have been extensively studied are the electrically addressed (EA-SLMs) and optically addressed (OA-SLMs) spatial light modulators. These are illustrated in Figure 1. To address an SLM implies that a signal is sent to modify the SLM properties at the pixel level. For the EA-SLM, a signal voltage is typically applied to a pixel electrode which results in a modification of the material's optical properties proportional to the applied voltage. A "read" beam of light incident on the material is thus spatially modulated in its intensity, phase, or both. The EA-SLM can be either transmissive or reflective. In an OA-SLM a spatially modulated beam, called the "write" beam, spatially modifies the material's optical properties, either directly or indirectly, in proportion to the write beam's intensity. A read beam, not necessarily of the same wavelength, interrogates the modulated material, resulting in a spatially modulated beam (usually reflected) that carries the same information as the write beam.

Bragg gratings have been proposed for use in SLMs[1] in situations where one can take advantage of their strong wavelength selectivity and highly efficient coupling of light into a single diffraction order. These gratings consist of a periodic modulation of the index of refraction in a material. If the index of refraction can be strongly modulated on a pixel

---

[*]sutherlandr@saic.com

1

level, then a Bragg grating can form an efficient EA-SLM or OA-SLM. Liquid crystals are often the material of choice for such a device because of their large birefringence which can be easily modulated. We have extensively investigated such liquid crystal based Bragg gratings in our laboratories. We have studied the dynamic properties of these gratings by electrical, thermal, and optical stimulation. Modification and control of optical and dynamic properties have been obtained through combinations of liquid crystals with polymers, combinations of various dopant materials, and interactions of liquid crystals with organic and inorganic interfaces. In this paper we present recent results on three types of Bragg gratings that we have studied: electrically switchable liquid crystal-polymer composites, thermally tunable cholesteric liquid crystals, and hybrid nematic liquid crystal-photorefractive crystal devices. We discuss the materials, fabrication, characterization, and physics of liquid crystal Bragg gratings and present some potential applications.
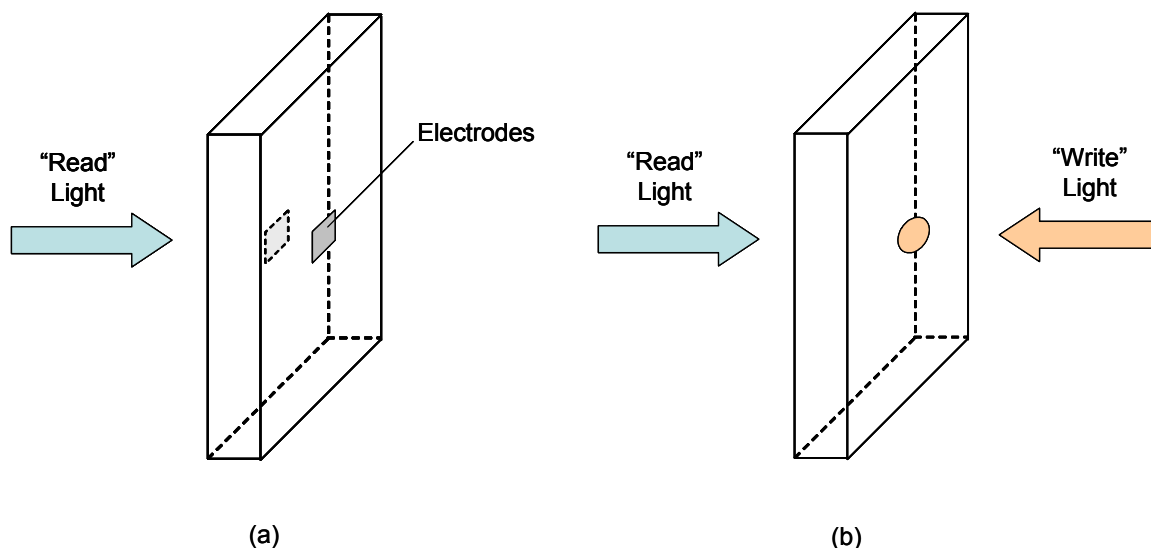
Figure 1. Schematic diagram of spatial light modulators. (a) EA-SLM. (b) OA-SLM.

2. SWITCHABLE COMPOSITE LIQUID CRYSTAL-POLYMER BRAGG GRATINGS

2.1. Holographic Polymer-Dispersed Liquid Crystals

For several years we have been studying holographic polymer-dispersed liquid crystals (HPDLCs) for switchable Bragg grating applications. These materials consist initially of a homogeneous mixture of monomer, liquid crystal (LC), and photointiator dye (and, in some cases, additional materials). The mixture is sandwiched between two transparent electrodes, and a hologram is written in the material. Monomer is preferentially polymerized in the bright regions of the optical interference pattern, while liquid crystal diffuses to the dark regions. When the miscibility gap is breached, liquid crystal phase separates into domains. The index contrast between the polymer and liquid crystal provides the modulation to create a Bragg grating. These domains can be reoriented by an applied electric field. At some field value the index of the liquid crystal matches that of the surrounding polymer, and the grating is switched off.

An advantage of using HPDLCs for switchable Bragg gratings is that complex holograms can be recorded in these materials, in addition to simple sinusoidal gratings, and hence many additional applications are possible, such as switchable flat, diffractive lenses with built-in aberration corrections. We will focus here on reflection gratings.

Thiol-ene-based reflective HPDLCs have recently been demonstrated to have substantial diffraction efficiency and good switching properties.[2] This is a simple three (or four[3]) component material system, consisting primarily of thiol-ene monomer and liquid crystal, with a small amount of initiator (and possibly a co-initiator[3]) which is consumed in the photochemical reaction, and hence the grating should be environmentally robust. The phase-separated liquid crystal domains (droplets) in this material are highly spherical and distinct. Hence the morphology of this material leads to incoherent or diffuse scattering as well as Bragg diffraction. Scattering can be a major issue in some applications.

We have studied the coherent diffraction and random scattering in thiol-ene-based HPDLC reflection gratings using a 2 × 2 matrix method and an effective medium theory.[4] The model incorporates realistic interfacial roughness and index inhomogeneities present in liquid crystal monolayer-droplet type gratings. Key parameters in the model are identified with morphological and optical properties of the grating. These include directly measurable parameters such as average droplet diameter, droplet diameter standard deviation, optical period, sample thickness, and refractive indices of the liquid crystal and polymer as functions of wavelength. Indirect or fitting parameters include volume fractions of droplets in high index regions and liquid crystal remaining in solution within the low index regions. Agreement of the model with experimentally measured transmission spectra of gratings at different Bragg wavelengths is excellent. The major impact of scattering is a reduction in the baseline transmittance, especially in the blue region of the spectrum, but it produces only a minor reduction in the diffraction efficiency at the Bragg wavelength. The predominant contribution to scattering loss is index inhomogeneity, and the inclusion of index dispersion for all material constituents is crucial to obtain agreement with data in the blue end of the spectrum.

Some key findings from this study are that the diffraction efficiency and scattering loss can be simultaneously improved by shaping the LC droplets and increasing the volume fraction of phase-separated LC. The index inhomogeneity in this system has two contributions: 1) droplet separation by polymer material, and 2) random orientation of droplet symmetry axes. The first contribution can be minimized by increasing the volume fraction of droplets, while the second is minimized by ordering the droplet symmetry axes in the grating plane. These effects will also increase the index modulation of the grating, at lease for one polarization of light, and hence increase the diffraction efficiency. The key is to stretch the droplets, i.e., to deform and coalesce them into LC "needles".

Our approach to achieving this is to shear the holograms in a direction perpendicular to the grating vector. Although this approach has been tried before,[5] our technique is different in that we incorporate an *in situ* shear during the optical recording.[6] We thus take advantage of some of the properties of the thiol-ene system. Since LC droplets are formed in this system by liquid-liquid instead of liquid-gel demixing, the system is fluid and allows significant deformation of the LC droplets. However, the system is also sufficiently viscous that the shear is easily transmitted from the boundary windows to the middle of the developing film. The key is timing the shear to occur during the optimal phase of the material during the photocure. When fully cured, the film locks in the droplet deformation.

2.2. Experiment

The liquid crystal BL037 was mixed in Norland NOA65 at an LC concentration of 35.5% by weight with a 2.0 wt-% concentration of the UV initiator Irgacure 4265. The mixture was then sandwiched between two indium-tin-oxide-coated glass slides using various spacers. Reflection gratings were recorded using a prism geometry.[2] The angle of incidence of 364-nm radiation from an Ar-ion laser was varied to control the Bragg wavelength of the hologram. Intensity incident on the sample was ~ 120-140 mW/cm^2, and the exposure time was varied.

Figure 2 shows the device and optical setup for shearing experiments. A linear shear deformation is produced in an HPDLC sample by sliding the glass sides of a sample cell past each other in a parallel direction. Since the formation of an HPDLC filter is a dynamic process, the timing of the shear during the grating formation is studied. The computer controlled motor allows the shear to be accomplished anytime during the formation process, while the shutter controls stops the exposure during the shear. A white light probe and a fiber spectrometer capture the notch formation and shear effects during the whole process of writing, shearing, writing, and releasing. Samples cured without shearing were also studied while applying a post-cure shear. Spectra were taken as the shear was applied.

Transmittance spectra of the sheared (either *in situ* or post-cured) HPDLC gratings were obtained by directing an unpolarized white-light source at the sample at normal incidence and collecting the transmitted light with an optical fiber connected to an Ocean Optics spectrometer. Each spectrum was normalized to the transmittance of a bare piece of glass to factor out air-glass Fresnel reflection losses. A linear polarizer allows for collection of transmission spectra of light polarized parallel to and perpendicular to the shear direction.

For TEM studies, cured holographic films were embedded in flat molds using Epo-fix resin and cured overnight in a 60 °C oven. The blocks were trimmed and ultramicrotomed at room temperature using an RMC Ultramicrotome. Sections of 50-60 nm thickness were cut with a 35° Diatome diamond knife, picked up onto 400-mesh hex Cu grids and vapor

stained with RuO_4. The sections were then imaged using bright-field TEM in an FEI CM200 transmission electron microscope. Images were obtained of varying magnifications between 5,000× and 50,000×.
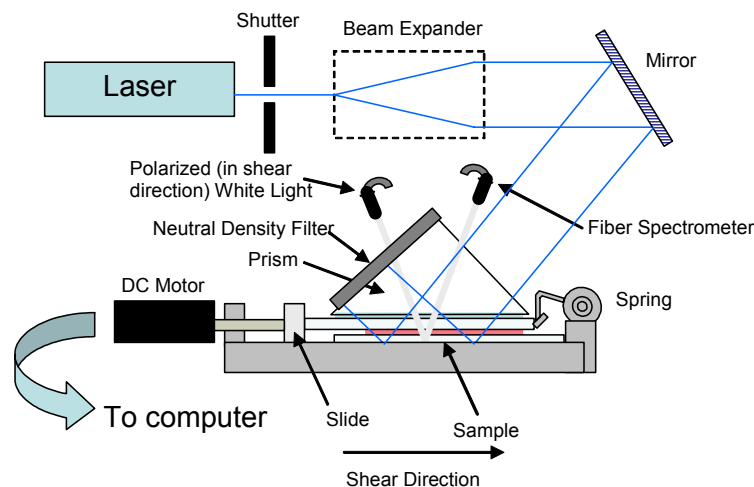
Figure 2. Schematic diagram of holographic recording apparatus incorporating *in situ* sample shear.

2.3. Results and Discussion

The response of HPDLC samples with varying cell thickness of 5, 8, 15, and 20 μm subjected to shear deformation only after curing was studied. Shear stress was applied to the samples while monitoring the transmission spectrum for light polarized in both the parallel and perpendicular directions to the shear. The electric field required for switching was measured for some samples while the films were under shear deformation. Also examined were the effects of applying a thin film of the thiol-ene (cured, uncured and gelled) to the glass surfaces before cell construction.

As the shear stress increases, the notch minimum decreases for polarization parallel to the shear deformation (i.e., higher diffraction efficiency) while the notch minimum for light polarization perpendicular to the shear increases. At higher shear, the perpendicular curve approaches zero and the parallel curve continues to increase approximately linearly. This is in agreement with previous similar work on this type of dependence of HPDLC reflection gratings.[5] No permanent deformation is apparent when releasing the shear force. The slides actually seem to slip across the film without losing optical contact.

Thin films of thiol-ene were spin-coated onto glass slides used for cell construction in an attempt to increase the bond strength between the film and the slides, thus reducing slippage and increasing the maximum shear. Films were treated in one of three ways before cell construction. Gelled samples were not exposed to UV light prior to filling. Oligomerized samples were exposed to UV light for 5 seconds (partially cured), and the polymerized samples were exposed to UV light for 45 seconds (fully cured). Coated cells yield a larger decrease in notch transmission for a given shear than the uncoated cell and result in lower attainable minimum notch depth (higher diffraction efficiency). Samples coated with a gelled thiol-ene performed the best with no lag between shear displacement and observed transmission notch decrease. Of the coated samples, polymerized coatings did the worst with similar results for the uncoated sample.

Sample thickness can also affect the shearing characteristics of the film. As sample thickness increases, diffraction efficiency goes up as usual, as well as the threshold value for notch deformation and the shear required for the notch to disappear in the perpendicular polarization. This might be explained by a non-uniform shear within the film from slide to slide, with thicker films showing a larger variation throughout the thickness.

The *in situ* shearing apparatus was modified to eliminate slippage of the driving actuator and an external dial micrometer was used to verify the shearing displacement. We show in Figure 3a the results of a sample subject to shear deformation *in situ*. Note the polarization dependence. For polarization perpendicular to the shear the diffraction efficiency is zero. On the other hand, the diffraction efficiency for light polarized parallel to the shear is nearly 99%. This is the highest diffraction efficiency we have observed in an HPDLC reflection grating. The baseline transmittance is also im-
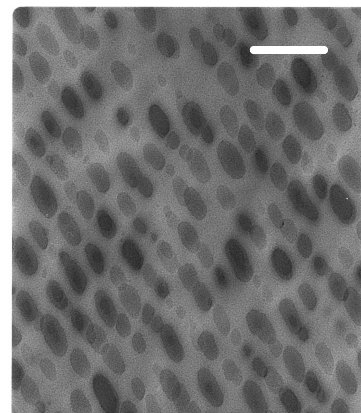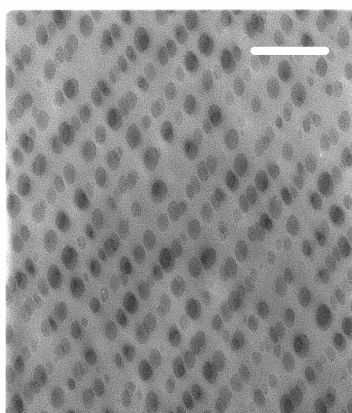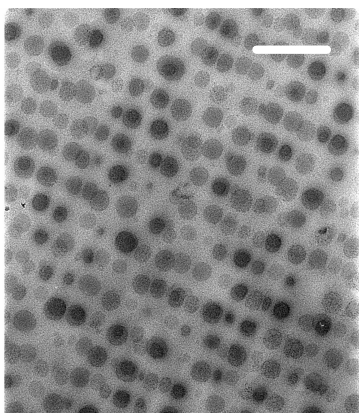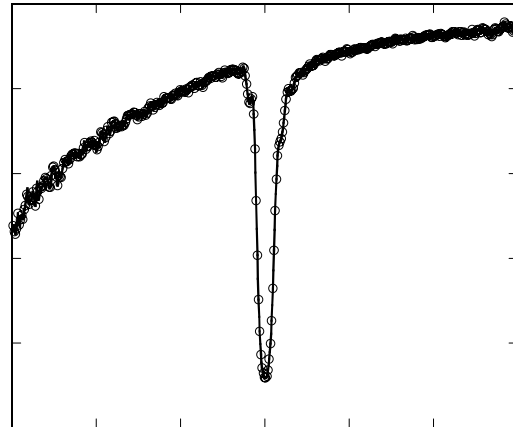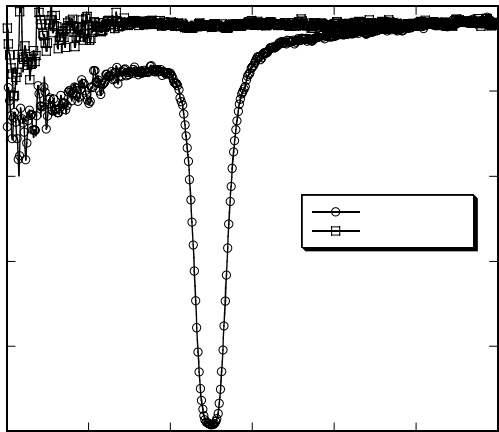
We have performed some preliminary studies of the electric fields required for switching these films. The required switching field decreases for light polarized perpendicular to the shear direction and increases for light polarization in the shear direction. The larger the shear, the greater the difference in switching field. However, the critical field for switching has not increased dramatically. We are continuing these studies.

3. TUNABLE CHOLESTERIC LIQUID CRYSTAL BRAGG GRATINGS

3.1. Cholesteric Liquid Crystal (CLC) Bragg Gratings

The cholesteric LC (CLC) in these studies consists of a nematic LC doped with a chiral agent. In any given plane, the molecules exhibit nematic orientational order. However, steric hindrances prohibit molecules in contiguous planes from achieving the same average orientation. Hence, the average orientation direction is slightly rotated from layer to layer. The sense of rotation is the same in each layer, resulting in a periodic twist of the average nematic orientation through the bulk of the liquid. The sense of the rotation depends on the chiral agent, and both right-handed and left-handed twists are possible.

The twist is linearly proportional to z, and the natural twist rate is q_0. This rate is determined by the concentration of the chiral dopant. A wide range of q_0 is possible. The distance along z over which the twist angle goes through a 360° rotation is called the pitch p_0, where $p_0 = 2\pi/q_0$. The total twist angle Φ in a cell with these chiral-doped LCs depends on the natural twist rate, the cell thickness, and boundary conditions at the confining substrates. The actual twist rate q and pitch p may differ slightly from the natural values.

When the pitch is such that $p \sim \lambda$, where λ is an optical wavelength, a single domain CLC will exhibit selective Bragg reflection over the wavelength range $n_o p < \lambda < n_e p$. Light polarized along the local director sees a refractive index n_e, while light polarized perpendicular to this direction sees n_o. For light propagating along the z axis, the normal modes of propagation in this inhomogeneous medium can be computed exactly in terms of Bloch waves.[7] The normal modes are elliptically polarized, in general. In the Bragg regime ($n_o p < \lambda < n_e p$), the wavevector of one mode is purely imaginary, which corresponds to an evanescent wave. This mode cannot propagate in the medium. The other normal mode is almost circularly polarized with the opposite handedness of the CLC helix.

Hence the CLC is a Bragg grating, for the proper handedness of incident polarized light, and in the Bragg regime it acts as a reflection filter. The incident light is not necessarily one of the normal modes. If the birefringence is not too large, so that $(n_e)^2 - (n_o)^2 << (n_e)^2 + (n_o)^2$, then the wave propagation can be analyzed using coupled-wave theory.[7] The field inside the CLC is taken to be a superposition of incident and reflected waves with wavevectors $\pm k$ given by

$$k = \frac{2\pi}{\lambda} \sqrt{\frac{n_e^2 + n_o^2}{2}} \tag{1}$$

If a left-hand circularly polarized wave is incident on a CLC with a left-handed twist (or, conversely, a right-hand circularly polarized wave incident on a right-handed CLC), then the wave is reflected with an efficiency R given by

$$R = \frac{\kappa^2 \sinh^2 sL}{s^2 \cosh^2 sL + (\Delta k/2)^2 \sinh^2 sL}, \tag{2}$$

where

$$s^2 = \kappa^2 - (k - q)^2, \tag{3}$$

$$\Delta k = 2(k - q), \tag{4}$$

$$\kappa = \frac{\frac{1}{\sqrt{2}} \pi (n_e^2 - n_o^2)}{\lambda \sqrt{n_e^2 + n_o^2}}. \tag{5}$$

The filter efficiency has the same form for the HPDLC Bragg reflection grating. However, for unpolarized incident light, the CLC filter has a peak reflection efficiency of

$$R^{\text{peak}}_{\text{unpolarized}} = \tfrac{1}{2}\tanh^2 \kappa L .$$ (6)

Thus, to obtain high rejection efficiency for unpolarized light, two CLC filters of opposite handedness in tandem are required.

3.2. Tunable CLC Filters

The Bragg wavelength of the CLC filter is given by $\lambda_{\text{B}} = \bar{n} p$, where $\bar{n}$ is the average refractive index. Hence to tune the filter, one can change the average refractive index or the pitch. A convenient way to do both is to apply an electric field. However, this results in reorientation of the molecular axis along the direction of the field, which reduces the amount of extraordinary index seen by the optical wave. From Eq. (5), we can see that this reduces the coupling coefficient and hence the diffraction efficiency. At some voltage the CLC will abruptly untwist and exist in a homeoptropic nematic state. This is sometimes referred to as a cholesteric-nematic transition. In the homeotropic state the selective Bragg reflection is destroyed. When the voltage is turned off, the cell attempts to return to the twisted CLC condition. Typically, though, this transition proceeds through an intermediate state, what is known as the focal conic state. In this state there are multiple domains of CLC with helical axes approximately parallel to the substrates. At domain boundaries the azimuth angle of the helix changes abruptly. This produces strong light scattering. The return to the single domain CLC state usually takes a very long time (minutes to hours or days).

The above effects are undesirable for SLM applications. Some techniques have been developed to alleviate these effects, such as adding a small amount of polymer to the CLC to stabilize the cholesteric state. Patterning the polymer holographically has been demonstrated to offer sufficient elastic memory to the grating to return the electrically perturbed molecules to their original orientation while lowering the switching voltage and improving the baseline scattering.[8] However, the problem of a reduction in coupling efficiency with applied field is still evident. A more desirable approach would be to gently unwind the CLC helix without reorienting the molecules.

The pitch depends on the concentration of chiral dopant. This concentration can be controlled thermally, which allows a simple tuning of the Bragg wavelength. Work demonstrating this has been reported using a left-handed CLC twist in medium with a positive dielectric anisotropy.[9] We have discovered an analogous effect in a left-handed medium with a *negative* dielectric anisotropy. We describe next our experiments with this type of Bragg grating.

3.3. Experiment

Cholesteric cells were made by mixing the chiral dopant S811 with nematic liquid crystals having negative dielectric anisotropy. Nematic LCs ZLI 2806 and ZLI 4788 were chosen for this study. The chiral dopant concentration was varied from 20% to as high as 60% in the mixture. Windows of the CLC cells were pretreated with an alignment layer formed by mechanical rubbing. The alignment is such that the helical axis is perpendicular to the rubbing direction. Cell thickness was set by using 10 or 15-μm spacers. For some studies, one of the cell windows was coated with a thin layer of pre-cured NOA65 doped with 1 wt-% of the broadband absorber nigrosin.

The spectrum of the CLC cell was measured using an unpolarized white light source in conjunction with an Ocean Optics spectrometer. Two types of experiment were performed. In one, the cell was housed in a hot stage and the temperature of the cell was varied. In the second, the nigrosin cell was irradiated with a Kr-ion laser at 647 nm. Nigrosin is well known as a heat transfer dye and has absorption from 420 nm to 700 nm.

3.4. Results and Discussion

A blue shift of the Bragg grating is expected as the chiral dopant concentration in the mixture is increased due to a tightening of the helical structure. We show in Figure 5 a plot of the Bragg wavelength as a function of chiral dopant concentration for a cell at 55 °C (35 wt-% S811 in ZLI 2806). At room temperature, however, the Bragg wavelength was in the red end of the spectrum for all concentrations of chiral dopant and, depending on the concentration of the dopant, a red shift was observed. Interestingly, the Bragg wavelength did not correlate with the chiral dopant concentration at room temperature, and no such systematic trend was evident.
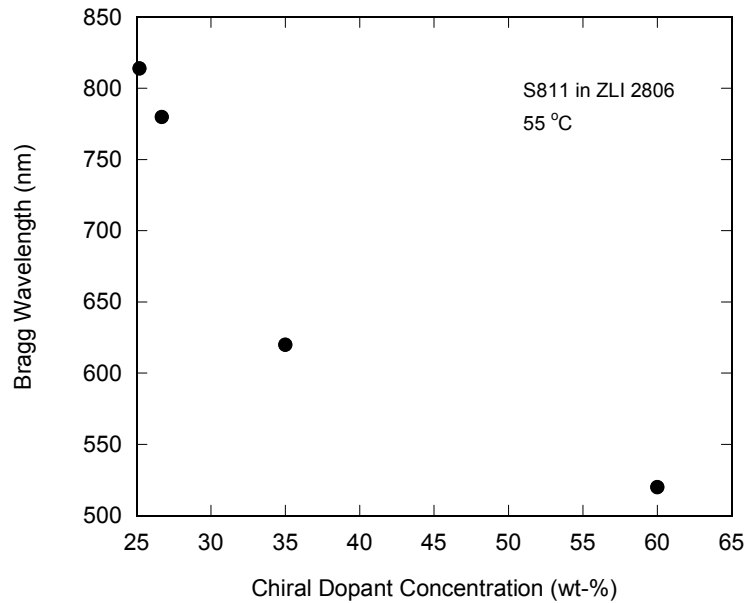
Figure 5. Bragg wavelength as a function of chiral dopant concentration at 55 ºC.

When heated on the hot stage there was, however, a progressive blue shift of the Bragg wavelength. The spectra at various temperatures are given in Figure 6. At room temperature the solubility of the chiral dopant is very low, and therefore the filter notch is seen at much longer wavelengths. The optical quality of the cells at room temperature was good. It is likely that microcrystals due to aggregation of the chiral dopant are formed on top of the nematic LC, and on heating more of the chiral material goes into solution.[9] This would explain the progressive blue shift with temperature. We have not, however, been able to observe any aggregates using polarized optical microscopy. We do note, though, evidence of a smectic A phase at room temperature. We are presently continuing our study of this phenomenon to ascertain the physics and chemistry of the thermally induced blue shift.
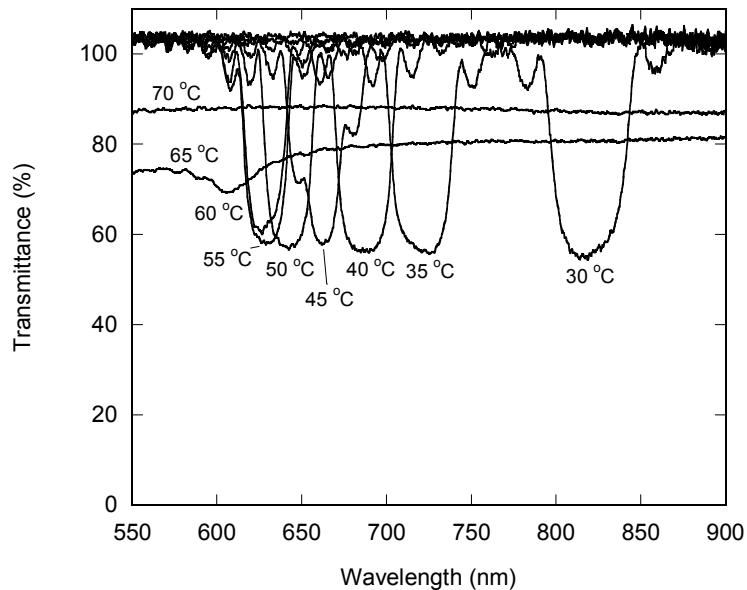

Figure 6. Thermal tuning of a CLC Bragg grating.

The maximum solubility of the chiral dopant is reached at ~ 55-60 °C. At temperatures > 60 °C degradation of the cell sets in. It is interesting to note that, on cooling, the Bragg wavelength red shifts and reaches its original position at room temperature. Very little hysteresis is observed during this heating and cooling cycle (Figure 7).
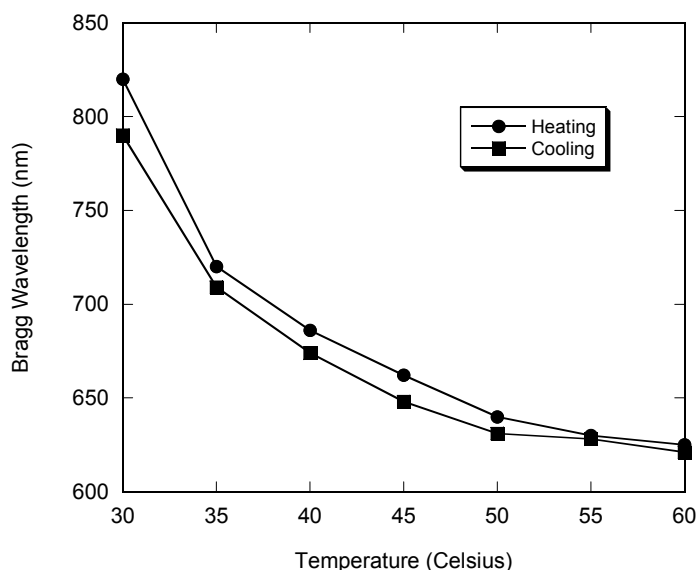

Figure 7. Bragg wavelength of CLC vs. temperature for heating and cooling cycles.

Thermal energy can be coupled into the CLC by optical absorption. To test this we originally doped the liquid crystal directly with an absorbing dye. Preliminary investigations confirmed this opto-thermal tuning of the Bragg wavelength, but results were obscured by the deep absorption notch of the visible dye. To obtain a more neutral, broadband absorption we then dissolved a small amount of nigrosin in the LC. The solubility of this dye is poor, but we did achieve a rather broadband absorption with about 1-2% absorption at the Kr-ion laser wavelength. This was enough to observe ~ 20-nm tuning under high optical power. To improve the tuning range, we finally developed a cell with a thin coating of doped Norland NOA65 on one window in direct thermal contact with a 10-μm thick CLC. The absorption of the nigrosin-doped NOA65 film at 647 nm was approximately 0.2. Figure 8 shows a time sequence of filter spectra for an optical loading of ~ 100 mW/cm^2 at 647 nm. A tuning range of > 100 nm is evident. The laser is turned off after 40 seconds, and the wavelength red shifts as the sample cools. An even larger tuning range (> 300 nm) can be obtained at higher power. Figure 9 gives the Bragg wavelength as a function of time when the laser intensity is ~ 425 mW/cm^2. The last data point on the plot corresponds to cooling of the sample after the laser is turned off.

4. HYBRID ORGANIC-INORGANIC DYNAMIC BRAGG GRATINGS

4.1. Two-Beam Coupling in Dynamic Bragg Gratings

For three decades the photorefractive effect has been studied in inorganic electro-optic crystals for applications that rely on an exchange of energy in a variety of nonlinear wave-mixing processes.[10] In a typical experiment two optical beams incident on a photorefractive material write a grating, due to the generation of a periodic space-charge field inducing an index modulation via the Pockels effect, and the grating is phase-shifted from the interference grating that induces it. Light is subsequently scattered from this grating. In this two-beam coupling process, unidirectional transfer of energy allows a weak signal beam to grow exponentially with distance, ultimately limited by the effects of depletion of the strong pump beam. For inorganic crystals the exponential gain coefficient is generally in the range of 10 to 100 cm^{-1}.

In recent years dramatic advances in the photorefractive properties of liquid crystals have been reported. Owing to the very high refractive index modulation possible using liquid crystals, coherent beam interactions can be pronounced, and this makes liquid crystals attractive media for the amplification of weak optical signals. Small signal gain coefficients as large as 2890 cm^{-1} have been reported using dye doped nematic liquid crystals in which the local molecular alignment was modulated using an internally generated space charge field from direct photo excitation.[11] Even higher gain coeffi-

cients of up to 3700 cm^{-1} have been reported from devices which use photo-generated space charges developed in photoconducting layers to modulate the alignment of adjacent undoped liquid crystals.[12,13] Operation of these devices has been restricted to the Raman-Nath regime, leading to multiple diffracted orders. Recent work has shown that large liquid crystal gain coefficients can be achieved in the Bragg regime when the space charge field originates from inorganic photorefractive crystals used as windows for undoped nematic liquid crystal cells.[14,15] The large effective trap density in the inorganic photorefractive media enables the surface space charge field to avoid saturation effects at the fine grating spacing necessary for Bragg-regime two-beam coupling in a thin layer of liquid crystal. The space-charge field penetrates the LC layer causing the nematic molecules to reorient. This produces a periodic index modulation, i.e., a Bragg grating.
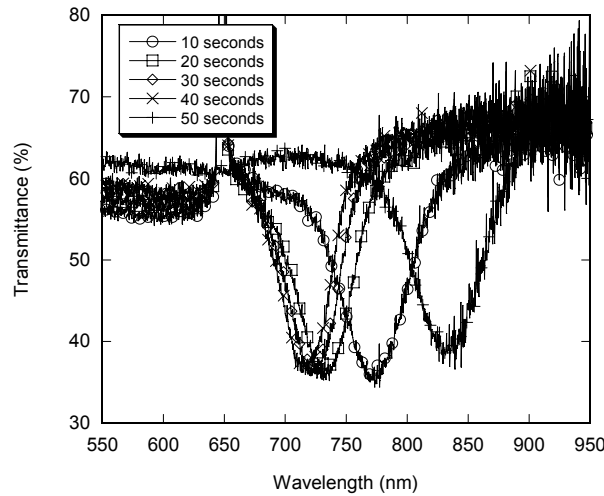

Figure 8. Opto-thermal tuning of a CLC Bragg grating with a Kr-ion laser at ~ 100 mW/cm^2. Plots show spectra at various times after initial irradiation of sample.
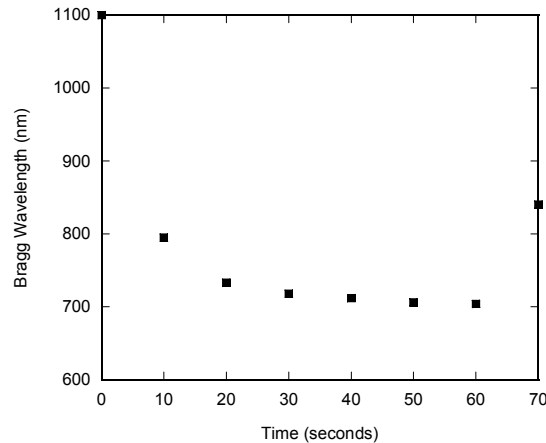

Figure 9. Bragg wavelength vs. time for opto-thermal tuning with a Kr-ion laser at ~ 425 mW/cm^2.

In order for hybrid organic-inorganic devices to work properly, the liquid crystal molecules should be sensitive to the sign of the local space charge field. Large gain can be attributed to the occurrence of a pre-tilt of the liquid crystal molecules at the inorganic window surfaces, leading to an induced molecular polarity through the flexoelectric effect.[16] Here we report the direct measurement of this pre-tilt angle and the two-beam coupling gain in these hybrid cells.

4.2. Experiment

Two uncoated inorganic crystals of strontium barium niobate doped with 0.01 weight % cerium (Ce:SBN 60) were used as windows for our liquid crystal cell. The windows were optically polished with finished dimensions of 20 mm × 20 mm × 1.31 mm. The crystal *c*-axis was parallel to one of the 20-mm long edges. The crystals were poled in our laboratory to create a single ferroelectric domain by heating each window above the Curie temperature for SBN (approxi-

mately 75 °C) followed by gradual cooling to room temperature in the presence of an externally applied electric field of 3 kV/cm.

Once poled and cleaned, the inside surface of each window was spin-coated at 4000 rpm for 30 seconds with a nylon multipolymer (DuPont Elvamide® 8023R, prepared as a 0.125 weight % solution in anhydrous methanol). After drying at room temperature for approximately 1 hour, the nylon coated cells were uniaxially rubbed using a nylon roller rubbing machine to induce a planar alignment of the liquid crystals. Rubbing directions both parallel and perpendicular to the c-axis of the SBN were employed.

The liquid crystal TL205 was mixed with a very small quantity of 8-μm or 10-μm glass rods to act as spacers for the assembled cell. The rods were dispersed thoroughly throughout the liquid crystal volume using an ultrasonic bath. A drop of the liquid crystal containing the dispersed spacers was placed onto the surface of one of the rubbed Ce:SBN windows. The cells with Ce:SBN windows were then filled with the LC by capillary attraction.

The hybrid cell was placed in a typical two-beam coupling experiment, with the two beams derived from the same cw 532-nm laser. The crossing angle was varied to vary the grating spacing in the sample. Pump beam and signal beam intensities at the input to the cell were approximately 160 mW/cm^2 and 56 μW/cm^2, respectively. A power meter was used to monitor the transmitted pump and signal powers. The measured gain is defined as the power of the signal with the pump present divided by the transmitted signal power in the absence of the pump. To factor out the gain due to the SBN windows, the gain was also measured by replacing the LC in the cell with an oil of similar index to the ordinary index of TL205. The gain coefficient is then given by $\Gamma = d^{-1}\ln(G)$, where G is the small signal gain due to just the LC, and d is the thickness of the LC layer.

The experimental arrangement for measuring the liquid crystal pre-tilt is described in Ref. 16. The experimental method is identical to that described originally by Baur et al.[17], and used by others as well[18,19], although here we have replaced the conventional glass-window liquid crystal cell with a hybrid photorefractive cell. The cell was situated between two crossed polarizers with axes oriented at ±45º with respect to the vertical axis of rotation. The cell was rotated about the crystal a-axis or c-axis using a calibrated rotation stage while the transmitted laser power through the analyzer was measured. A 3-mW polarized He-Ne laser operating at 594 nm was used for this experiment.

4.3. Results and Discussion

The problem of finding the field components transmitted by the analyzer in the cell rotation experiment in terms of the incident field components, and therefore the transmission of the system, was analyzed in detail using the extended Jones matrix method as described in Ref. 16. A fit of the data to the theoretical transmittance $T(\theta,\theta_c,d)$, where θ is the angle of incidence, θ_c is the pre-tilt angle, and d is the LC thickness, yields the value of the pre-tilt angle.

The experimental parameters for the Ce:SBN crystals are $n_{wo} = 2.33$, $n_{we} = 2.30$, $\alpha_{wo} = 0.052$ cm^{-1}, and $\alpha_{we} = 0.089$ cm^{-1}, where the subscript w implies parameters for the windows. For the liquid crystal TL205, $n_o = 1.527$ and $n_e = 1.744$. The liquid crystal thickness is not accurately known and we allow for some variation over the sample. The pre-tilt angle θ_c is not known *a priori* and must be determined by fitting the theoretical transmittance to experimentally measured data. To analyze the data, we performed a two-parameter (θ_c and d) fit to the data using the *genfit* function in MathCad 11, which employs a Levenberg-Marquardt algorithm. This function performs a least-squares fit to the nonlinear function $T(\theta,\theta_c,d)$ and requires the partial derivatives $\partial T/\partial\theta_c$ and $\partial T/\partial d$ as well as an input guess-vector $(\theta_{c,\text{guess}},d_{\text{guess}})^{\text{T}}$.

We have performed experiments on samples with the rubbing direction parallel and perpendicular to the c-axis of the windows. Results of pre-tilt angle measurements are shown in Figure 10. Although the parallel rubbed sample shows a larger pre-tilt, there is some variation of this over the sample. The average pre-tilt angle lies somewhere between the two values determined by the data in these two plots. (Note that the sign of the pre-tilt angle is not significant, but only reflects an arbitrary definition of a positive or negative angle of incidence.) These pre-tilt angles are substantial; measurements taken with simple glass cells made using the same fabrication method yield a pre-tilt that is typically less than 1°. Therefore, if parallel rubbed SBN windows are used to construct an LC cell, the director should exhibit a significant amount of splay, leading to a relatively large flexoelectric effect.
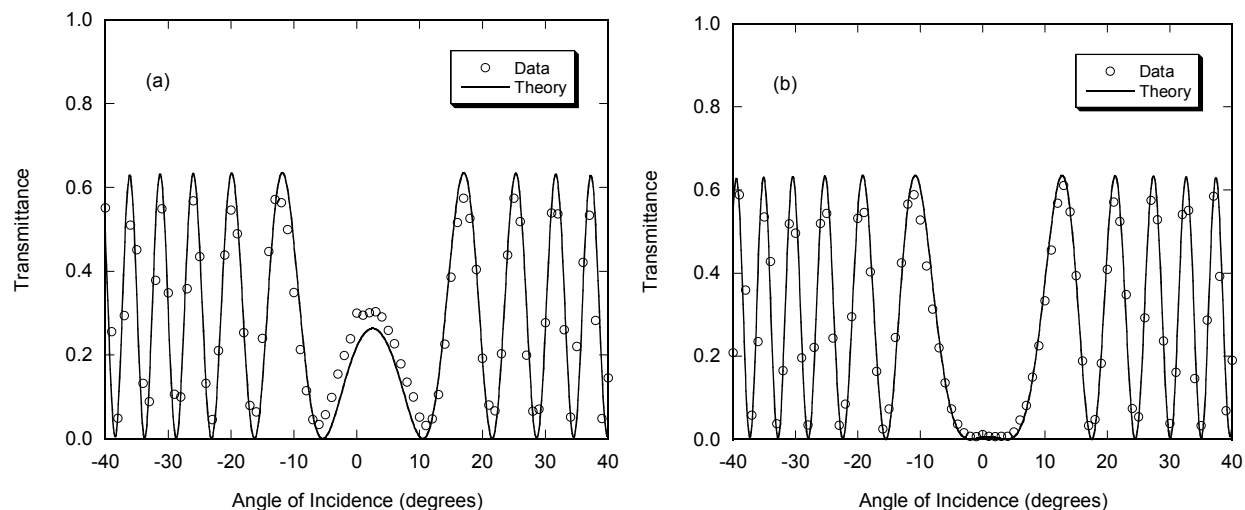
Figure 10. Fits of cell rotation data to theory. (a) Rubbing || c-axis. Fit parameters: $\theta_c = 13.2º$, $d = 9.1$ μm. (b) Rubbing || a-axis. Fit parameters: $\theta_c = -6.5º$, $d = 7.5$ μm.

Figure 11 shows the results of two-beam coupling gain measurements for the parallel and perpendicularly rubbed cells. The peak gain coefficient occurs at a grating spacing of ~ 1.5 μm for both types of cell, close to the optimum grating spacing for beam coupling in Ce:SBN alone, where the space charge field is largest. For both types of cell, parallel alignment of the rubbing directions for the two opposing windows yields the largest gain. This is in agreement with the pre-tilt measurements, which as noted lead to large director splay. The flexoelectric effect induces a molecular polarity because parallel rubbing in the presence of a pre-tilt causes the planar aligned molecules to become splayed, squeezing together the ends of the molecules and causing a tiny displacement of the electron cloud in each LC molecule. This induced polarity is necessary to satisfy the conditions for unidirectional gain in the hybrid cell.[15] The gain coefficients represented in Figure 11 are larger by at least a factor of 4 than those of the best inorganic material.
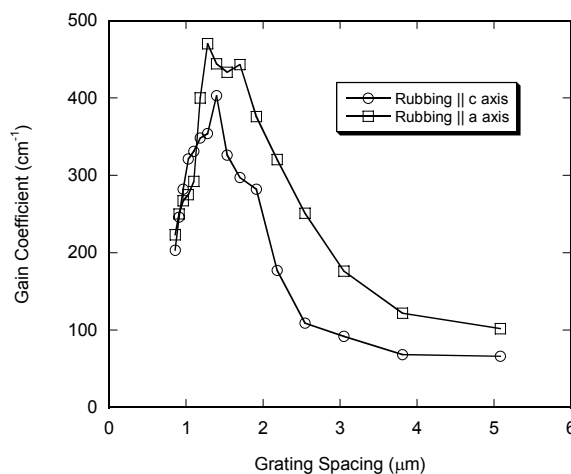

Figure 11. Two-beam coupling gain coefficient vs. grating spacing for hybrid LC-photorefractive cell for two different rubbing directions.

5. APPLICATIONS

One of the most obvious areas of application for HPDLC EA-SLMs is in digital displays, such as consumer TVs, office projectors, and cinema. An early innovation, developed to the prototype stage, was an electronic color filter wheel to replace the mechanical filter wheel in projectors.[20] This consisted of a stack of five HPDLC Bragg reflection gratings, each reflecting a different color band from a white light source in time sequence. We note that the newly developed

sheared thiol-ene HPDLCs have a higher diffraction efficiency and, because of a simpler three-component material system, may be more robust in the high temperature, high intensity environment of a video projector.

To make the HPDLC Bragg grating function as a true EA-SLM requires only pixelating the electrodes as in standard LCDs. A stack of red, green, and blue gratings could then function as a full color display for TVs, cell phones, camera viewers, etc. Another approach is to combine a stack of HPDLC Bragg gratings with an ordinary LCD to make a display that functions well indoors, with an ordinary backlight, and outdoors, reflecting bright ambient light.[21] Note that these applications will make use of the electronically controlled variable diffraction efficiency (i.e., "gray" scale) of HPDLCs.

Devices that make use of the binary on-off switching of HPLDC Bragg gratings at a single wavelength are also of interest. One of these is for optical data storage. A computer can write a digital "page" of data to an HPDLC EA-SLM in the form of a spatial array of on-off voltages. A coherent beam reading these data will then be spatially modulated with a 2D array of binary data, 0's and 1's (i.e., dark and light pixels), either on reflection or transmission. This beam can then be interfered with another coherent beam to write a hologram in an optical storage medium. In optical communications, a stack of different HPDLC EA-SLMs can function as an array of wavelength-selective switches to control signals in fiber-optic lines. Such a stack could also be used as a wavelength selective attenuator, in the variable diffraction efficiency mode, to balance the power levels of all channels in a fiber and thus act as a dynamic gain equalizer.

The opto-thermally tunable CLC Bragg grating can function as an OA-SLM. An incoherent image projected onto an absorbing thin film can be converted into a coherent image by interrogating the CLC side of the SLM with a laser near the Bragg wavelength. A similar type of configuration could be used for up-converting an IR image to a visible image. Several image processing applications are then possible. A thermally tunable notch filter could be used in telecom applications to selectively block specific DWDM (dense wavelength division multiplexed) channels while letting other channels pass.

The hybrid LC-photorefractive cell can also function as an OA-SLM. Two schemes to do this are using a four-wave mixing scheme in a hybrid cell where an image has been projected onto the cell, or using a simple real-time holography setup where a sinusoidal amplitude grating is superimposed on the image projected onto the cell.[22] In both of these cases, the output read beam bears the image as a spatial intensity modulation. Another approach which does not require beams incident at a single Bragg angle is to simply project an image onto the hybrid cell. The cell responds to the spatially varying image intensity with spatial modulations to the refractive index, forming a complex phase image. A coherent read beam propagating collinearly through this phase image carries the image information as a spatial phase modulation.

6. CONCLUSIONS

In summary, liquid crystal based Bragg gratings offer much potential for use in spatial light modulators. We have described three different types of liquid crystal Bragg grating that we are studying in our laboratories: switchable HPDLC reflective gratings, tunable CLC filters, and hybrid liquid crystal-photorefractive Bragg gratings. *In situ* shearing of thiol-ene HPDLCs has led to higher diffraction efficiency (approaching 99%) and much improved baseline scattering. Transmission electron micrographs lend support to a theory that we are elongating the liquid crystal droplets in a direction substantially along the grating plane. In CLC gratings we have discovered that an unusually large concentration of chiral dopant can substantially red-shift the Bragg wavelength at room temperature, whereas low concentrations cause a blue shift. The chiral dopant solubility can then be controlled thermally to tune the Bragg wavelength toward the blue end of the spectrum. We have shown in a negative dielectric anisotropy liquid crystal that this can be controlled optically by also doping the sample with a broadly absorbing dye, making such a Bragg grating suitable for optically addressed spatial light modulators. Finally, we have also demonstrated a hybrid dynamic grating by combining a nematic liquid crystal with photorefractive windows, and have shown that a large induced pre-tilt angle in these types of cells is responsible for the two-beam coupling by establishing a large splay in the liquid crystal director leading to a strong flexoelectric effect. Since the gain in this hybrid cell is at least a factor of 4 larger than the best inorganic photorefractive medium, the hybrid cell may be the optimum choice for replacing inorganic media in many photorefractive spatial light modulator applications.

ACKNOWLEDGEMENTS

REFERENCES

1. R. L. Sutherland, L. V. Natarajan, V. P. Tondiglia, R. T. Pogue, S. A. Siwecki, D. M. Brandelik, B. L. Epling, E. Berman, C. Wendel, and M. G. Schmitt, "Holographic PDLCs for spatial light intensity modulation," Proc. SPIE **3633**, 226 (1999).
2. L. V. Natarajan, C. K. Shepherd, D. M. Brandelik, R. L. Sutherland, S. Chandra, V. P. Tondiglia, D. Tomlin, and T. J. Bunning, "Switchable holographic polymer dispersed liquid crystal reflection gratings based on thiol-ene photopolymerization," Chem. Mater. **15**, 2477 (2003).
3. L. V. Natarajan, D. P. Brown, J. M. Wofford, V. P. Tondiglia, R. L. Sutherland, P. F. Lloyd, and T. J. Bunning, "Holographic polymer dispersed liquid crystal reflection gratings formed by visible light initiated thiol-ene photopolymerization," Polymer **47**, 4411-4420 (2006).
4. R. L. Sutherland, V. P. Tondiglia, L. V. Natarajan, P. F. Lloyd, and T. J. Bunning, "Coherent diffraction and random scattering in thiol-ene–based holographic polymer-dispersed liquid crystal reflection gratings," J. Appl. Phys. **99**, 123104 (2006).
5. M. Date, Y. Takeuchi, K, Tanaka, and K. Kato, "Reflectivity improvement in holographic polymer dispersed liquid crystal (HPDLC) reflective display devices by controlling alignment," IEICE Trans. Electron. (Japan) **E81-C**, 1685-1690 (1998).
6. R. L. Sutherland, L. V. Natarajan, V. P. Tondiglia, and T. J. Bunning, "Switchable Volume Hologram Materials and Devices," U. S. Patent 6,699,407 B1 (2004).
7. P. Yeh and C. Gu, Optics of Liquid Crystal Displays (John Wiley & Sons, New York, 1999).
8. E. R. Beckel, L. V. Natarajan, V. P. Tondiglia, R. L. Sutherland, and T. J. Bunning, "Electro-optic properties of holographically patterned, polymer stabilized cholesteric liquid crystals," submitted for publication.
9. Y. Huang, Y. Zhou, C. Doyle, and S. -T. Wu, "Tuning the photonic band gap in cholesteric liquid crystals by temperature-dependent dopant solubility," Opt. Express **14**, 1236-1242 (2006).
10. L. Solymar, D. J. Webb, and A. Grunnet-Jepssen, The Physics and Applications of Photorefractive Materials (Clarendon Press, Oxford, 1996).
11. I. C. Khoo, B. D. Guenther, M. V. Wood, P. Chen, and M. -Y. Shih, "Coherent beam amplification with a photorefractive liquid crystal," Opt. Lett. **22**, 1229-1231 (1997).
12. F. Kajzar, S. Bartkiewicz, and A. Miniewicz, "Optical amplification with high gain in hybrid-polymer-liquid-crystal structures," Appl. Phys. Lett. **74**, 2924-2926 (1999).
13. S. Bartkiewicz, K. Matczyszyn, A. Miniewicz, and F. Kajzar, "High gain of light in photoconducting polymer–nematic liquid crystal hybrid structures," Opt. Commun. **187**, 257-261 (2001).
14. G. Cook, C. A. Wyres, M. J. Deer, and D. C. Jones, "Hybrid organic-inorganic photorefractives," Proc. SPIE **5213**, 63-77 (2003).
15. G. Cook, J. L. Carns, M. A. Saleh, and D. R. Evans, "Substrate induced pre-tilt in hybrid liquid crystal/inorganic photorefractives," Mol. Cryst. Liq. Cryst. **453**, 141-153 (2006).
16. R. L. Sutherland, G. Cook, and D. R. Evans, "Determination of large nematic pre-tilt in liquid crystal cells with mechanically rubbed photorefractive Ce:SBN windows," Opt. Express **14**, 5365-5375 (2006).
17. G. Baur, V. Wittmer, and D. W. Berreman, "Determination of the tilt angles at surfaces of substrates in liquid crystal cells," Phys. Lett. **56**, 142-144 (1976).
18. T. J. Scheffer and J. Nehring, "Accurate determination of liquid-crystal tilt bias angles," J. Appl. Phys. **48**, 1783-1792 (1977).
19. K. Han, T. Miyashita, and T. Uchida, "Accurate determination and measurement error of pretilt angle in liquid crystal cell," Jpn. J. Appl. Phys., Part 2 **32**, L277-L279 (1993).
20. R. Smith, M. Popovich, and S. Sagan, "Application specific integrated lenses and filters for microdisplays using electrically switchable Bragg grating technology," Proc. SPIE **4207**, 31-38 (2000).
21. K. Sumiyoshi, and H. Hayama, "Liquid Crystal Display Device Having Switchable Reflective Layer," US Patent 6,842,209 B2 (2005).
22. P. Yeh, Introduction to Photorefractive Nonlinear Optics (John Wiley & Sons, New York, 1993).